Long-range laser ranging using superconducting nanowire single-photon detectors

Li Xue (薛 莉)[1,*], Ming Li (李 明)[1], Labao Zhang (张蜡宝)[2,], Dongsheng Zhai (翟东升)[3], Zhulian Li (李祝莲)[3], Lin Kang (康 琳)[2], Yuqiang Li (李语强)[3], Honglin Fu (伏红林)[3], Ming Ming (明 名)[4], Sen Zhang (张 森)[2], Xu Tao (陶 旭)[2], Yaoheng Xiong (熊耀恒)[3], and Peiheng Wu (吴培亨)[2]**

[1]*Key Laboratory for Space Object Measurements, Beijing Institute of Tracking and Telecommunications Technology, Beijing 100094, China*

[2]*Research Institute of Superconductor Electronics, Nanjing University, Nanjing 210093, China*

[3]*Yunnan Observatory, Chinese Academy of Sciences, Kunming 650011, China*

[4]*Changchun Institute of Optics, Fine Mechanics and Physics, Chinese Academy of Sciences, Changchun 130033, China*

**Corresponding author: xuelishirley@sjtu.edu.cn; **corresponding author:lzhang@nju.edu.cn*

Received February 26, 2016; accepted April 15, 2016; posted online May 20, 2016

We demonstrate laser-ranging results for non-cooperative targets at ranges of 237 m and 19 km using superconducting nanowire single-photon detectors (SSPD). We upgrade the kilohertz rate laser-ranging system with a newly developed SSPD module, and the equivalent detection diameter is enlarged to 50 μm with a fiber and micro-lenses. Both retroreflectors and non-cooperative surfaces of aluminum foil, a solar panel, and a concrete panel at distances of 237 m and 19 km, whose echoes are of single-photon level, are ranged with sub-centimeter precision. Experimental signal-to-noise ratio curves with the product of quantum efficiency and system transmittance are obtained, which indicates that our system, with an average laser power of 0.8 W and a receiving aperture of 1.2 m, may be capable for space debris ranging at a distance of 800 km. This work suggests that SSPDs have the potential to be used for space debris surveillance.

OCIS codes: 280.3400, 120.0280, 040.5570, 120.1880.
doi: 10.3788/COL201614.071201.

Laser ranging is the most accurate technique currently available to determine the range of space targets, and it has made significant contributions to satellite tracking, lunar measurements, three-dimensional laser imaging, and geophysics research[1–4]. Most previous work on laser ranging has been performed using single-photon avalanche detectors (SPADs). However, SPADs suffer from low quantum efficiency, a high dark count rate, and low overall repetition rate, which limit its application to long-range non-cooperative targets with low echo levels[5,6]. Superconducting nanowire single-photon detectors (SSPDs) have rapidly emerged as a highly promising single photon detector since 2001[7]. SSPDs have undergone significant improvements and received considerable attention due to their wide response bandwidth (0.4–2 μm), low dark count rate (<100 cps), and high repetition rate (~100 MHz), enabling numerous impressive applications such as quantum communications[8–11], optical communications[12,13], fluorescence spectrum[14], laser ranging and imaging[15–20]. In 2007, Warburton *et al.* for the first time advocated sub-centimeter depth profiling for retroreflectors at a distance of 330 m using SSPDs[17]. Afterwards, Chen *et al.* further enhanced laser imaging for non-cooperative targets at a distance of 2.5 m based on SSPDs[18]. More recent studies made significant advances for cooperative satellites at a distance of 3000 km[19] and for non-cooperative targets at a distance of 910 m[20], respectively. However, the number of echoes from non-cooperative targets is usually low, and laser-ranging experiments for non-cooperative targets using SSPDs are currently carried out at distances of no longer than several hundred meters. Up to now, there have been few reports about laser ranging using SSPDs for non-cooperative targets at kilometer-level distances or even for space debris.

In this Letter, we report a new development in laser ranging for non-cooperative targets obtained with an SSPD. Using a newly designed SSPD and the receiving optics in the upgraded system, both cooperative and non-cooperative targets at distances of 237 m and 19 km are successfully ranged. Experimental and theoretical signal-to-noise ratio (SNR) curves indicate that our system, with an average power of 0.8 W and a receiving aperture of 1.2 m, has the potential for space debris ranging at 800 km.

The designed SSPD module is a key device in our laser ranging system, which is shown in Fig. 1. The nanowire is made from niobium nitride (NbN) with a film thickness of 5 nm, a detection area of 12 μm × 12 μm, and a very effective and broadband detection spectrum from the visible to the infrared band. Operated at the bias current of 6 μA, the dark count rate of the SSPD is less than 100 cps, and the timing jitter and the dead time are 50 ps and 20 ns, respectively. A novel technology using a multi-mode fiber (core diameter: 50 μm, numerical aperture: 0.22) and micro-lens (object distance: 7 mm, image distance: 2.8 mm, confocal length: 2 mm)[21] enlarges the equivalent

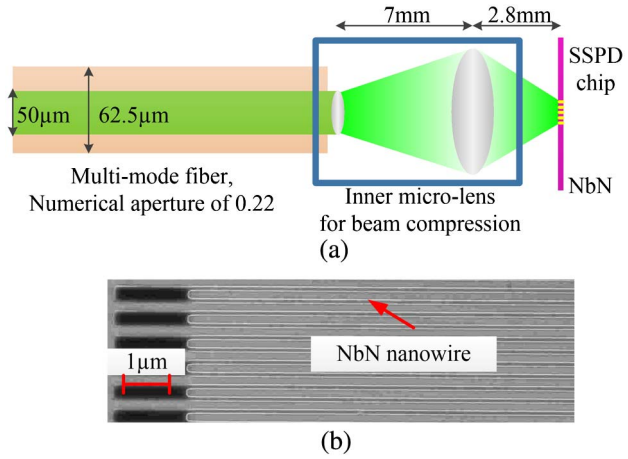

Fig. 1. SSPD used in the experiments. (a) Optical design. (b) Image taken by scanning electron microscope.

detection diameter of the SSPD module to 50 μm. The nominal coupling efficiency of 87% can be obtained based on the coupling optics.

The receiving optics are designed with two main considerations: one is the allowed focus spot size, and the other is the allowed divergence angle of the incident light from the multi-mode fiber. As shown in Figs. 2 and 3, the equivalent focal length of the designed receiving optics is about 2.52 m, and the aperture of telescope is about 1.2 m. Thus, the corresponding divergence angle is about 11.4°, consistent with the allowed divergence angle of the multi-mode fiber (12.7°). In the experiments, a collimated reference light propagating through the receiving optics is first used for calibration. The diameter of the focus spot on the front side of the fiber is about 30 μm, which meets the requirements of the core diameter of fiber (50 μm). The laser powers before and after propagating through the multi-mode fiber are detected. The input reference laser power is about 40 μW, while the output laser power after propagation is about 33 μW, which indicates a fiber coupling efficiency of 80%. Along with the efficiency (~70%) of the telescope, a total coupling efficiency of near 50% from the telescope optics to the detector through the multi-mode fiber can be expected.

During the experiments, the SSPD is fiber packaged and mounted in a cryocooler operating at a temperature of 2 K. An afocal 1.2 m-aperture telescope transmits 1 kHz repetition rate laser pulses (average laser power: 0.8 W, full width at half-maximum: <100 ps) towards the targets, and a small percentage of the transmitted laser is split to provide a starting event. Both the cooperative retroreflector and the non-cooperative targets, including aluminum foil, a solar panel, and a concrete panel, are chosen as the targets in the experiments. In order to directly demonstrate the long-range ranging capability of SSPDs, targets are placed at a distance of 19 km with an atmospheric transmittance of about 0.1. Experiments are also carried out at a distance of 237 m with an atmospheric transmittance of about 0.5, which is much closer to the atmospheric conditions for space targets. Laser pulses reflected by the targets go through the same optics and are coupled into the multi-mode fiber after collimation, beam compression, and filtering. A photon event detected by the SSPD is logged as an ending event, and the target range is determined from the time difference between the starting and ending events. During the experiments, a gating functionality is provided to reduce the external noise. Additionally, the attenuators are adjustable with a transmittance from 0 to 80 dB, and the received photon intensity is cut down by the attenuators to reduce the number of echoes and noise to low level.

The photoelectric conversion is a classic Poisson process[22], and the probability that one or more photoelectrons are generated can be expressed as $P = 1 - P_0(n)$,

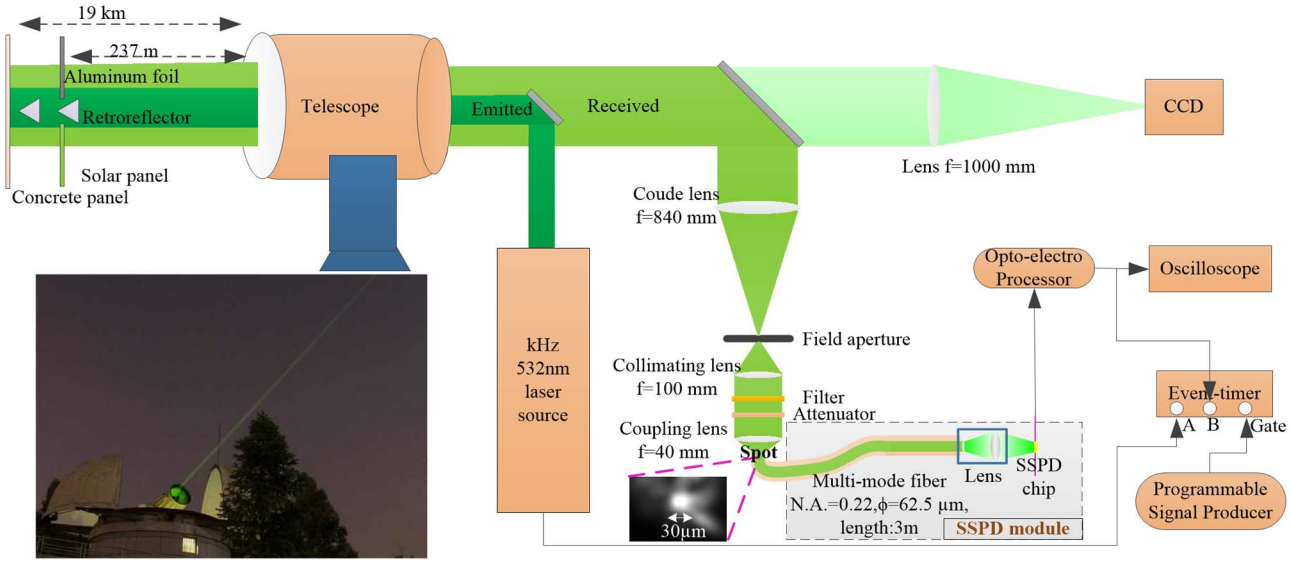

Fig. 2. Scheme of the coaxial optical system layout and laser-ranging experiments. The receiving optics are designed to meet the requirements of the allowed focus spot size and the allowed divergence angle of the incident light from the multi-mode fiber.

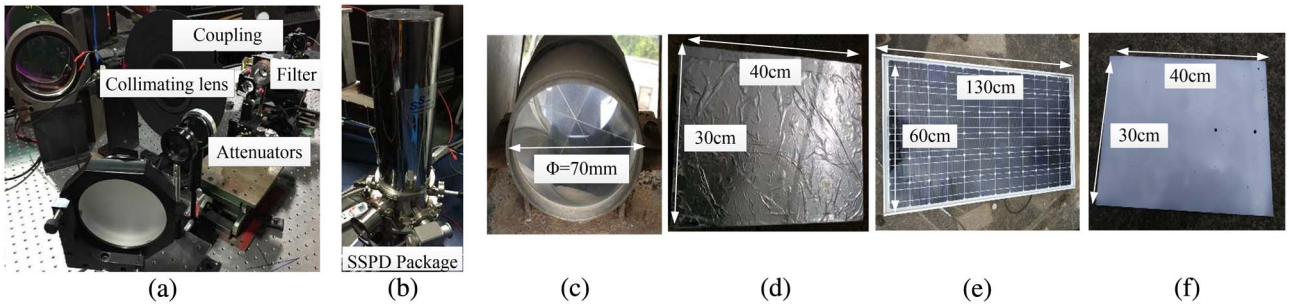

Fig. 3. Experimental setups. (a) Receiving optics, (b) the SSPD package, (c) the retroreflector, (d) the aluminum foil, (e) the solar panel, and (f) the concrete panel.

where $P_0(n) = \exp(-n)$ and n is the number of received photons. From the conversion, the echo number and noise number arrived at the detector per laser pulse can be derived from the logged echo number and noise number by SSPD. In our experiments, the initial number of echoes without attenuation is evaluated as about 0.015 for aluminum foil, 0.008 for the solar panel, and 0.0035 for the concrete panel, and the initial amount of noise during gating period is about 0.25. A retroreflector with an echo number of 10^4 and a noise number of 100 is set as a comparison.

Taking the aluminum foil at a distance of 237 m as an example, the process of target range determination is shown in Fig. 4. A range of 235 m can be estimated from the two peaks from the waveform on oscilloscope, as shown in Fig. 4(a). The statistical histogram is laid out in Fig. 4(b), where the peak centroid in the histogram is about 237 m. From the scattering diagram shown in Fig. 4(c), the echoes are statistically relevant, while the noises are randomly distributed. Thus, the target range of 237.170 m and the inner precision of 6.9 mm are extracted by polynomial fitting and 3σ iterations[23], with most of the noise struck out, as shown in Fig. 4(d). While the theoretical inner precision can be estimated from the timing jitter of the SSPD (50 ps), the laser pulse width (100 ps), atmospheric turbulence (100 ps), and target geometry depth (200 ps) based on the equation

$$\sigma = \sqrt{\sigma_{\text{jit}}^2 + \sigma_{\text{pul}}^2 + \sigma_{\text{tur}}^2 + \sigma_{\text{geo}}^2}, \tag{1}$$

where σ_{jit}, σ_{pul}, σ_{tur}, and σ_{geo}, which are about 1.25, 2.5, 2.5, and 5 mm, represent the corresponding contributions from the timing jitter, laser pulse width, atmospheric turbulence, and target geometry depth to the precision, respectively. It can be seen that the experimental precision is in good agreement with its theoretical value.

Another important metric in laser ranging is the SNR, which is defined from the statistical diagram as[24]

$$\text{SNR} = \frac{n_{\text{echo}}}{\sqrt{n_{\text{echo}} + n_{\text{noise}}}}, \tag{2}$$

where n_{echo} is the number of detected echoes in the target channel bin of the statistical diagram, including echoes from the target and the noise located within target

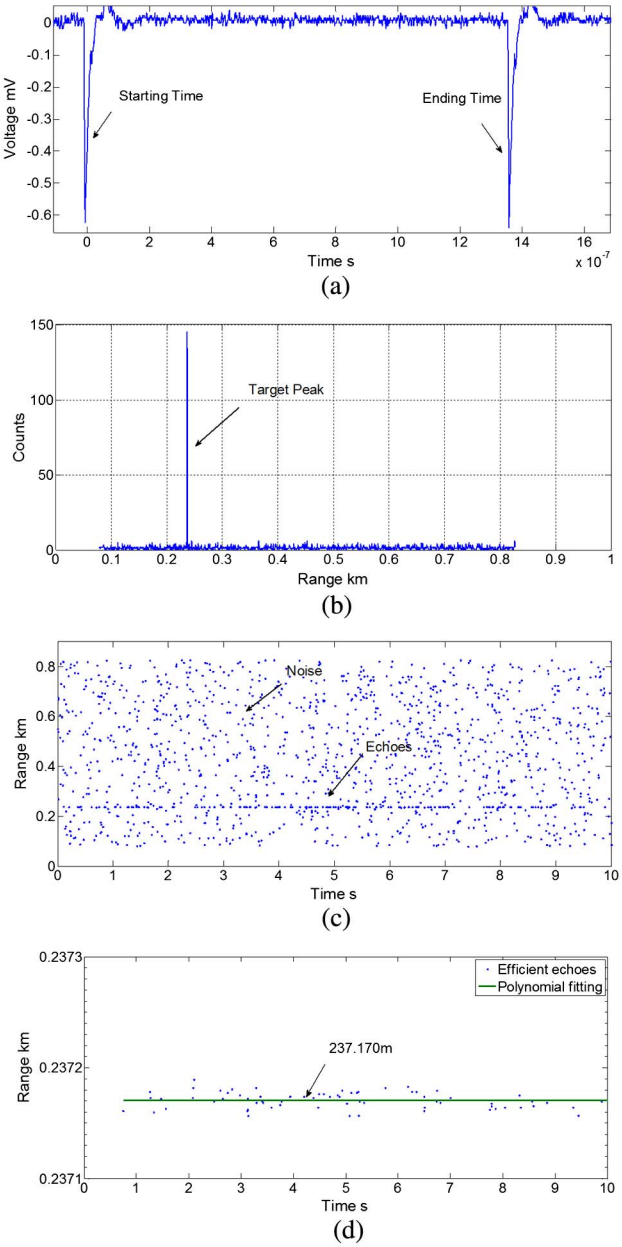

Fig. 4. Target range determination. (a) Starting and ending time from the waveform. (b) Target peak in statistical histogram. (c) Echo and noise distribution. (d) Polynomial fitting and 3σ iteration results.

Table 1. Ranging Results for Different Remote Targets

R (km)	Target	R_d (km)	σ (mm)	SNR
0.237	Retroreflector	0.237737	13.4	74.15
	Aluminum foil	0.237170	6.9	7.75
	Solar panel	0.236903	3.5	5.60
19	Retroreflector	19.021984	18.3	73.71
	Concrete panel	19.035666	23.2	4.02

broadening range, and n_{noise} is the detected average noise number per channel bin. Here, the bin length is decided by the dead time of the SSPD. Table 1 summarizes the ranging results for the retroreflectors and non-cooperative targets at distances of 237 m and 19 km. R is the standoff distance, R_{d} is the determined range, and σ is the ranging precision. The experimental precisions are consistent with the theoretical values evaluated from the system parameters according to Eq. (1). The experimental results successfully demonstrate the feasibility of long-range (tens of kilometers) laser ranging for retroreflectors and non-cooperative targets using SSPDs.

In order to further demonstrate the laser-ranging capability for space debris using SSPDs, an SNR model versus the product γ of the quantum efficiency and system transmittance is established. Firstly, the number of detected echoes n_{echo} in the target bin is estimated as

$$n_{\text{echo}} = N_{\text{p}} \cdot \frac{n_0}{n_0 \cdot \xi + n_{\text{dv}}} \cdot [1 - P_0(n_0 \cdot \xi + n_{\text{dv}})], \quad (3)$$

where n_0 is the number of echoes from the target per laser pulse, f_{rep} is the laser repetition rate (1 kHz), t_{mea} is the total measured time period (10 s), and $N_{\text{p}} = f_{\text{rep}} \cdot t_{\text{mea}}$ is the number of total laser pulses. Here, t_{dead} is the dead time of the SSPD (20 ns), t_{broad} is the broadened time of echoes according to Eq. (1), v_{ex} is the external noise rate (1000 cps), and v_{dark} is the dark count rate of the SSPD (100 cps). $v_{\text{noi}} = v_{\text{ex}} + v_{\text{dark}}$ is the total noise rate, $n_{\text{dv}} = t_{\text{dead}} \times v_{\text{noi}}$ is the noise number within the dead time, and $\xi = t_{\text{dead}}/t_{\text{broad}}$ is the fill factor of the dead time within the broadening time. The detected noise includes two parts: the noise in the target bin and the noise in the other bins. Thus, the amount of detected noise within the target bin is

$$n_{\text{noise}} = \frac{N_{\text{p}}}{N_{\text{bin}}} \cdot \frac{v_{\text{noi}}}{\frac{n_0}{t_{\text{broad}}} + v_{\text{noi}}} \cdot [1 - P_0(n_0 \cdot \xi + n_{\text{dv}})] + \frac{N_{\text{p}}}{N_{\text{bin}}} \cdot \left(\frac{t_{\text{gate}}}{t_{\text{dead}}} - 1\right) \cdot [1 - P_0(n_{\text{dv}})], \quad (4)$$

where t_{gate} is the gate period (9.5 μs) per laser pulse, and $N_{\text{bin}} = t_{\text{gate}}/t_{\text{broad}}$ is the number of bins. During the experiments, the quantum efficiency and the system transmittance are changed by adjusting the current bias applied to the SSPD and the transmittance of the attenuators. Thus, the number of the received echoes and noises can be expressed as

$$n_0' = \gamma \cdot n_0, \qquad v_{\text{noi}}' = \gamma \cdot v_{\text{noi}}, \qquad n_{\text{dv}}' = \gamma \cdot n_{\text{dv}}. \quad (5)$$

n_0, v_{noi} and n_{dv} are then replaced with n_0', v_{noi}', and n_{dv}' in Eqs. (3) and (4). Substituting the two equations into Eq. (2), the relationship between the SNR and the product γ of the quantum efficiency and the system transmittance can be obtained.

Experimental and theoretical SNR curves are obtained for the retroreflector, aluminum foil, and solar panel, as shown in Fig. 5. The SNR for the retroreflector first increases and then decreases with the increasing γ. This may be due to the fact that the echo number of the retroreflector is large, and the SSPD has no photon number resolution ability. Thus, when γ increases over the threshold value, the echo detection probability $1 - P_0(\gamma \cdot n_0)$ remains almost unchanged, while the increasing number of detected noise results in the reduction of the SNR. For the aluminum foil and solar panel with much fewer echoes, the SNR increases with γ, which is in good agreement with the theoretical curves. Therefore, a rough estimation of the minimum acceptable γ is estimated to be about 0.13, according to the empirical threshold SNR of 2 for echo recognition.

As the initial photon number echoes from the aluminum foil and solar panel are 0.015 and 0.008, respectively, the corresponding minimum number of echoes required in our system is about 0.001. Combined with the laser radar equation for non-cooperative targets[25], the number of received echoes by the detector can be expressed as follows:

$$n_0 = \frac{\lambda}{hc} \cdot E_{\text{t}} \cdot T^2 \cdot K_{\text{t}} \cdot K_{\text{r}} \cdot \frac{D^2 \rho S}{8\pi R^2 \left(\frac{D}{2} + \frac{R\theta_t}{2}\right)^2}, \quad (6)$$

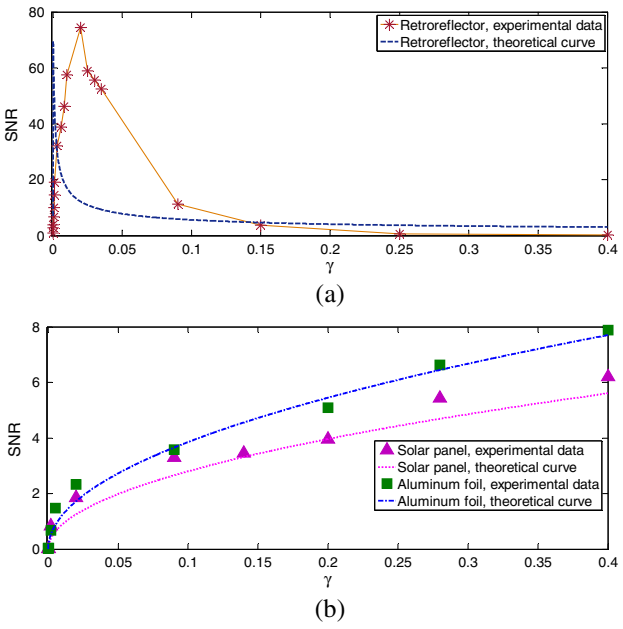

Fig. 5. Experimental and theoretical SNR curves for (a) retroreflector and (b) aluminum foil and solar panel.

where $\lambda = 532$ nm is the laser wavelength, $h = 6.626 \times 10^{-34}$ J · s is the Planck constant, and $c = 299792458$ m/s is the light speed. Here, $E_t = 0.8$ mJ is the pulse energy, $T = 0.5$ is the atmosphere transmittance, $K_t = 0.8$ and $K_r = 0.5$ are the optical system efficiencies of the transmitting and receiving system, S is the target equivalent area, $D = 1.2$ m is the telescope aperture, and $\theta_t = 10''$ is the laser divergence. Since n_0 is about 0.001, it means our system using an SSPD can approximately detect 1 m^2 space debris at a range of 800 km.

Using SSPD as a new detection module, the detection range for non-cooperative targets is improved to tens of kilometers. Moreover, the SNR curves indicate that our system, with an equivalent detection area of 50 μm, an average laser power of 0.8 W, and a receiving aperture of 1.2 m, has the capability for space debris laser ranging, opening up interesting application of SSPDs to space debris surveillance. With developed larger telescopes, higher laser power, smaller laser pulse widths, a lower dark count rate of the SSPD, and a closed-loop tracking system, laser ranging for smaller space debris at longer distances with higher precision can be expected in the future.

This work was supported by the National Natural Science Foundation of China (No. U1431116) and the National High Technology Research and Development Program of China (No. 2011AAXXX0110).

References

1. R. Devoti and V. Luceri, Geophys. Res. Lett. **28**, 855 (2001).
2. J. Lee, Y. J. Kim, K. Lee, S. Lee, and S. W. Kim, Nat. Photon. **4**, 716 (2010).
3. T. W. Murphy, Rep. Prog. Phys. **76**, 076901 (2013).
4. B. S. Sheard, G. Heinzel, K. Danzmann, D. A. Shaddock, W. M. Klipstein, and W. M. Folkner, J. Geodesy **86**, 1083 (2012).
5. M. D. Eisaman, J. Fan, A. Migdall, and S. V. Polyakov, Rev. Sci. Instrum. **82**, 071101 (2011).
6. C. M. Natarajan, M. G. Tanner, and R. H. Hadfield, Supercond. Sci. Technol. **25**, 063001 (2012).
7. G. N. Gol'tsman, O. Okunev, G. Chulkova, A. Lipatov, A. Semenov, K. Smirnov, and R. Sobolewski, Appl. Phys. Lett. **79**, 705 (2001).
8. H. Takesue, S. W. Nam, Q. Zhang, R. H. Hadfield, T. Honjo, K. Tamaki, and Y. Yamamoto, Nat. Photon. **1**, 343 (2007).
9. D. Rosenberg, A. J. Kerman, R. J. Molnar, and E. A. Dauler, Opt. Express **21**, 1440 (2013).
10. R. H. Hadfield, Nat. Photon. **3**, 696 (2009).
11. F. Kaiser, A. Issautier, L. A. Ngah, O. Alibart, A. Martin, and S. Tanzilli, Laser Phys. Lett. **10**, 045202 (2013).
12. R. Sobolewski, A. Verevkin, G. N. Gol'tsman, A. Lipatov, and K. Wilsher, IEEE Trans. Appl. Supercond. **13**, 1151 (2003).
13. B. Lu, F. Wei, Z. Zhang, D. Xu, A. Pan, D. Chen, and H. Cai, Chin. Opt. Lett. **13**, 091402 (2015).
14. C. M. Natarajan, M. G. Tanner, and R. H. Hadfield, Supercond. Sci. Technol. **25**, 063001 (2012).
15. Z. Zhao, G. Wen, B. Hui, and D. Li, Chin. Opt. Lett. **10**, 031001 (2012).
16. F. Yang, X. Zhang, Y. He, and W. Chen, Chin. Opt. Lett. **12**, 082801 (2014).
17. R. E. Warburton, A. McCarthy, A. M. Wallace, M. S. Hernandez, R. H. Hadfield, S. W. Nam, and G. S. Buller, Opt. Lett. **32**, 2266 (2007).
18. S. Chen, D. Liu, W. Zhang, L. You, Y. He, W. Zhang, X. Yang, G. Wu, M. Ren, H. Zeng, Z. Wang, X. Xie, and M. Jiang, Appl. Opt. **52**, 3241 (2013).
19. H. Li, S. Chen, L. You, W. Meng, Z. Wu, Z. Zhang, K. Tang, L. Zhang, W. Zhang, X. Yang, X. Liu, Z. Wang, and X. Xie, Opt. Express **24**, 3535 (2016).
20. A. McCarthy, N. J. Krichel, N. R. Gemmell, X. Ren, M. G. Tanner, S. N. Dorenbos, V. Zwiller, R. H. Hadfield, and G. S. Buller, Opt. Express **21**, 8904 (2013).
21. L. Zhang, M. Gu, T. Jia, R. Xu, C. Wan, L. Kang, J. Chen, and P. Wu, IEEE Photon. J. **6**, 1 (2014).
22. J. W. Goodman and P. L. Haupt, *Statistical Optics* (John Wiley & Sons, 2015).
23. L. Xue, M. Li, and L. Wang, Proc. SPIE **9297**, 92970C (2014).
24. S. Pellegrini, G. S. Buller, J. M. Smith, A. M. Wallace, and S. Cova, Meas. Sci. Technol. **11**, 712 (2000).
25. J. Dong and Q. Hu, Chin. Opt. Lett. **5**, S176 (2007).